FUNCTION™ american physiological society

FUNCTION, 2021, 2(4): zqab026

https://doi.org/10.1093/function/zqab026
Advance Access Publication Date: 10 May 2021
Evidence Review

EVIDENCE REVIEW

Bioengineered Kidney Models: Methods and Functional Assessments

Astia Rizki-Safitri[1,2], Tamara Traitteur[1,2,3], Ryuji Morizane [1,2,4,3,*]

[1]Nephrology Division, Massachusetts General Hospital, Boston, MA 02129, USA, [2]Department of Medicine, Harvard Medical School, Boston, MA 02115, USA, [3]Wyss Institute for Biologically Inspired Engineering, Harvard University, Cambridge, MA 02115, USA and [4]Harvard Stem Cell Institute, Cambridge, MA 02138, USA

*Address correspondence to R.M. (e-mail: rmorizane@mgh.harvard.edu)

Abstract

Investigations into bioengineering kidneys have been extensively conducted owing to their potential for preclinical assays and regenerative medicine. Various approaches and methods have been developed to improve the structure and function of bioengineered kidneys. Assessments of functional properties confirm the adequacy of bioengineered kidneys for multipurpose translational applications. This review is to summarize the studies performed in kidney bioengineering in the past decade. We identified 84 original articles from PubMed and Mendeley with keywords of kidney organoid or kidney tissue engineering. Those were categorized into 5 groups based on their approach: de-/recellularization of kidney, reaggregation of kidney cells, kidney organoids, kidney in scaffolds, and kidney-on-a-chip. These models were physiologically assessed by filtration, tubular reabsorption/secretion, hormone production, and nephrotoxicity. We found that bioengineered kidney models have been developed from simple cell cultures to multicellular systems to recapitulate kidney function and diseases. Meanwhile, only about 50% of these studies conducted functional assessments on their kidney models. Factors including cell composition and organization are likely to alter the applicability of physiological assessments in bioengineered kidneys. Combined with recent technologies, physiological assessments importantly contribute to the improvement of the bioengineered kidney model toward repairing and refunctioning the damaged kidney.

Key words: bioengineered kidney; tissue engineering; kidney organoids; organ-on-a-chip; kidney function; systematic review

Introduction

The kidney is an organ that plays a pivotal role in urine production. It consists of elaborate filtration, reabsorption/secretion, and collection units, making a reconstruction in vitro difficult. However, in vitro kidney models such as kidney organoids have already been bioengineered, including the successful recapitulation of the complex tissue of a native kidney, and applied to a wide range of renal preclinical investigations. Unlike conventional monolayer models, they consist of 3D self-assembled tissues in vitro that embody architectural and functional properties similar to in vivo kidneys.[1,2] In this regard, renal progenitor cells derived from pluripotent stem cells (PSCs) are commonly employed by virtue of their ability to differentiate into kidney epithelial cells in a self-organized fashion.[3–6] Other models, similar to organoids (organoid-like) but derived from adult cells, possess less pluripotency[7–11] or complexity,[8,12–17] yet exhibit the capacity to recapitulate kidney functions for various preclinical purposes, including disease modeling and drug testing.

Physiological properties of a kidney include functions to filtrate and reabsorb/secrete substrates for urinary excretion from the body. Endothelial cells composing renal tissues allow blood filtration in glomeruli and secretion/reabsorption in tubules.[18] Functional assessments that measure these physiological

Submitted: 31 December 2020; **Revised:** 4 May 2021; **Accepted:** 6 May 2021

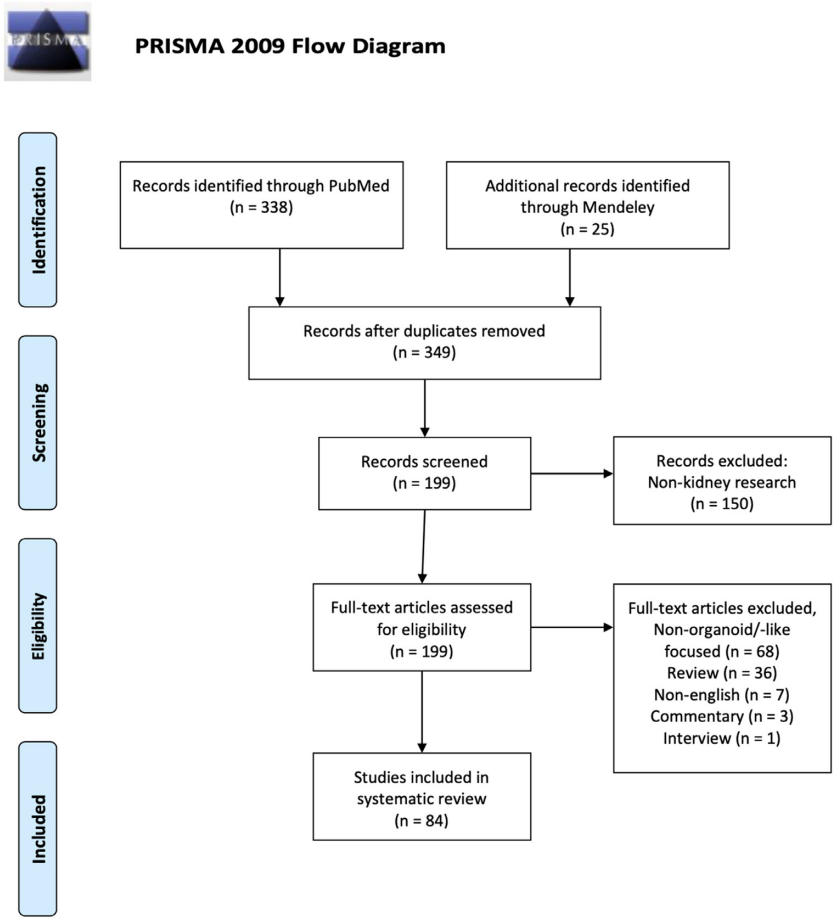

Figure 1. Screening Process on Selecting Reviewed Studies Using PRISMA Flow Diagram

characteristics in the native kidney have also been applied to bioengineered kidney models to study toxins, diseases, and regeneration.

Building kidney models does not only recapitulate the highly complex tissue of a native kidney but also resemble its physiology. However, many studies conducted in kidney models were not able to perform the same tests that usually assess renal function in vivo and are the standard in clinical studies. A reason why some of these functional assessments like creatinine clearance do not work might be found in the morphological discrepancy between the native kidney and kidney models. Thus, most assays applicable in bioengineered kidney tissues have been developed to evaluate cellular functions (eg, albumin uptake). Here, we review studies of kidney bioengineering and summarize the current approaches of kidney tissue models. We concurrently list and discuss the functional assessments conducted on bioengineered kidneys, suggesting implementations and improvements that could guide future research in producing efficient biologically relevant kidney models.

Materials and Methods

Articles were searched and collected from PubMed and Mendeley using the following keywords: (kidney organoid) OR (kidney AND tissue engineering) NOT (review) with [MeSH Terms] and [Publication Type]. Studies conducted within the past 11 years (January 1, 2010–March 30, 2021) were filtered. Using the described keywords, 338 and 25 studies were found in PubMed and Mendeley, respectively. We followed the preferred reporting items for systematic reviews and meta-analyses (prisma) flow diagram (Figure 1) to identify studies eligible for this review.[19] After removing duplicates, a total of 306 articles were included for further screening based on their relevance to kidney research. We excluded 150 articles that are not related to kidney research. Further, 115 articles were excluded based on multiple reasons: nonorganoid/-like focused (68 articles), review (36 articles), non-English (7 articles), commentary (3 articles), and interview report (1 article). We excluded nonorganoid/-like focused (68 articles) studies where the kidney models lacked all of the following criteria: (1) capacity to be self-organized (2) in a 3D structure (3) with multiple cell types, (4) ability to recapitulate organ development, and (5) functionality corresponding to native kidney.[6] Finally, 84 articles were eligible for review. Eight independent articles were added to complement the discussion on both kidney models and functional assessments.

Results and Discussion

Types of Bioengineered Kidney Models

From the 84 collected studies, we identified 5 different types of bioengineered kidney models based on the approaches: (1) decellularization and recellularization of kidney, (2) reaggregation of kidney cells, (3) kidney organoid, (4) kidney in scaffolds, and (5) kidney-on-a-chip (Figure 2). We summarized the culture

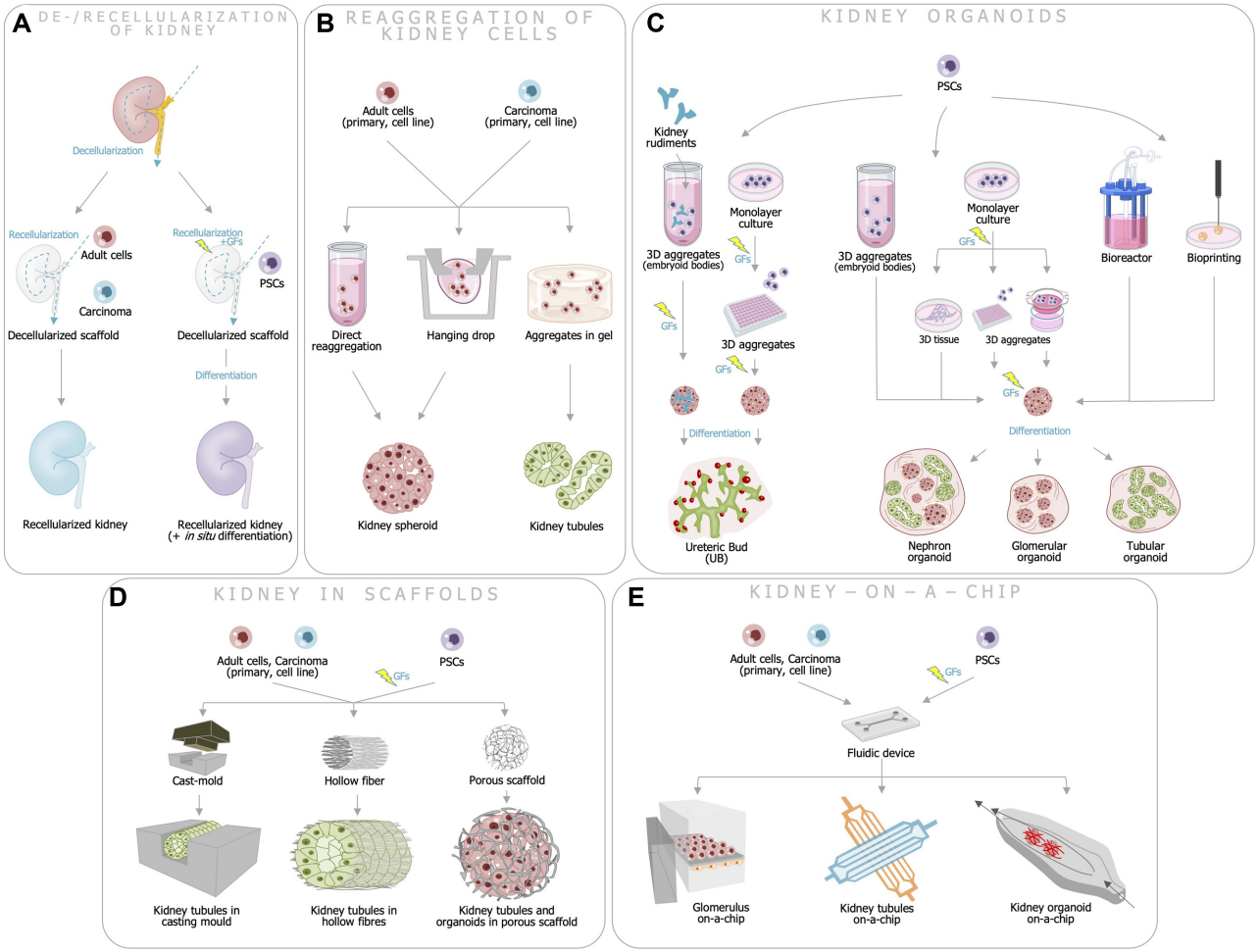

Figure 2. Types of Bioengineered Kidney Models and Techniques to Obtain the Models. **(A)** Decellularization and recellularization of kidney, **(B)** reaggregation of kidney cells using adult cells, **(C)** kidney organoid established from PSCs, **(D)** kidney in synthetic scaffolds, and **(E)** kidney-on-a-chip integrated with fluidic devices.

technique, cell sources, outcome (tissue characterization), and applications in Table 1.

Decellularization and Recellularization of Kidney

Eleven studies employed decellularization and recellularization of kidney to establish a kidney model in vitro. Here, inhabiting cells were eliminated from the extracellular matrix (ECM) of a native kidney leaving a scaffold that can be repopulated with nonnative kidney cells. Notably, this retained the innate 3D organization of kidneys. Exploiting various species like rodents,[7,20–22] porcine,[23–26] sheep,[27] and rhesus monkeys[28,29] resulted in varied sizes of decellularized scaffolds. Concomitantly, laboriousness of the de- and recellularization procedure increased with the complexity of the organisms used. In general, decellularization was accomplished by anionic detergents (eg, sodium dodecyl sulphate (SDS)[7,20,21,23,24,26,28] and Triton X[20,21,23,27]) that were perfused via the renal artery. Subsequently, primary embryonic renal cells and endothelial cells, kidney cell carcinomas, or PSCs were seeded for recellularization. Repopulation was accomplished with a recellularization rate of up to 90%, and cells were viable for 21 days.[24] After transplantation into a model organism, immune responses of host cells appeared to be somewhat decreased over time,[21,26] and host cells migrated into the recellularized grafts.[26]

The specific composition of the provided native ECM is assumed to play a pivotal role in supporting cell localization and 3D architecture during these processes. In detail, endothelial cells were found to specifically reside in the glomerular area upon repopulation[7,22] where particular types of collagen and laminin are distributed.[23] However, the laminin content of decellularized scaffolds was generally decreased as opposed to collagen and therefore appears to be more susceptible to corrosion during kidney decellularization.[30]

In addition, growth factors (GFs) are preserved in decellularized kidney scaffolds, most likely altering cell differentiation.[21,25,28,31] In particular, factors like insulin-like growth factor binding protein 7, epithelial growth factor-7,[28] hepatocyte growth factor,[21] and vascular endothelial growth factor (VEGF)[21,25] were found in decellularized scaffolds, which might have induced proliferation and differentiation of PSCs. A recellularization using PSCs without any GF-supplementation concomitantly demonstrated their differentiation into immature kidney cells in the decellularized scaffold.[28] However, a significant decrease in several GFs was observed during the decellularization process, including fibroblast growth factor (FGF),[25] transforming growth factor beta (TGF-β), and interleukin 8 (IL-8).[21] Less abrasive detergents like sodium deoxycholate during decellularization might retain higher levels of GFs.[25]

Table 1. Culture Techniques, Cell Sources, and Outcomes of Bioengineered Kidney Models

Type of Bioengineered Kidney	Techniques				Cell Sources		Outcomes		Application	Ref.
	Approach	Culture	Combined Method/s	Degree of Modulation*	Organism	Pluripotency	Cell/Tissue Composition	Cells Organization		
De-/recellularization of kidney	Decellularization and recellularization	Perfusion	• Renal artery perfusion with SDS • Fibroblast reprogramming into iPSC[7] • Transplantation[7,20,21,27] • Coculture with endothelial cells[20] • Addition of endothelial GFs: *Act.A, BMP4, RA, VEGF*[22]	Low–high	Rodents, Porcine, Sheep, Monkey, Human	*Adult cells:* Primary cortex, carcinoma	Whole kidney tissue	Simple complex of 3D tissue	• Cell therapy • Transplantation	[21,23,24,26,27,29]
					Mouse, Human	*PSCs:* mESCs, Reprogrammed patient-derived fibroblast, hESCs line (H9), hiPSCs line (Clone IV)	Whole kidney tissue, nephron endothelial cells resided in glomerular area	Simple complex of 3D tissue		[7,20,22,25,28]
Reaggregation of kidney cells	3D self-assembly	Direct aggregation into 3D culture	• Transplantation[9]	Low	Human	*Adult cells:* Primary cortex, Primary carcinoma	Mono-tissue, possibly multiple tissues	3D structure No distinct tissue organization[9] or organized in tubular structure[32]	• Personalized medicine • Disease modeling • Drug screening • Transplantation	[9,32]
		Hanging drop	-	Low	Human	*Adult cells:* Primary cortex	Possibly multiple tissues	3D structure No distinct tissue organization	Drug screening	[11,33]
		Aggregates in gel	• CRISPR/Cas9[10,16] • Viral infection[17] • Hydrogel fabrication[31,34] • Bioprinting[31] • Fluidic channel[16]	Low–moderate	Mouse, Human Mouse, Porcine	*Adult cells:* Urinary tubular cell, tubular cell line (RPTEC, HK-2), Tubular carcinoma (NKi-2) Mouse primary tubular cell, tubular cell line (LLC-PK1)	Mono-tissue: proximal tubule	3D structure organized in tubular structure	• Personalized medicine • Disease modeling • Drug screening • Transplantation	[8,10,12,13,16,17,31,34,35,36]
Kidney organoid (UB)	Differentiation of anterior IM using UB GFs: *CHIR, BMP, RA, FGF, YAP inhibitor*	Embryoid bodies	Coculture with kidney rudiment	Low–moderate	Mouse, Human	*PSCs:* mESCs (Hoxb7, Wt1, CD1) hiPSCs line (201B7), kidney rudiment	Wolffian duct Ureteric tree (branching)	Complex 3D structure with distinct tissue organization	Kidney development studies	[43–45]
		Adhesion and 3D culture	Embedded ECM culture	Low	Human	hESCs line (KhES-3, H1)				[43,46,53]

Table 1. Continued

Type of Bioengineered Kidney	Techniques				Cell Sources		Outcomes		Application	Ref.
	Approach	Culture	Combined Method/s	Degree of Modulation*	Organism	Pluripotency	Cell/Tissue Composition	Cells Organization		
Kidney organoid (nephron)	Differentiation of posterior IM using nephron GFs: *CHIR, FGF, Act.A, heparin*	In vivo differentiation	• Direct aggregation into 3D culture • Transplantation	Low	Mouse, Human	hAFSC PSCs: mESCs,	Podocytes Proximal tubules	Simple complex of 3D tissue	Kidney development studies	52
		Embryoid bodies	-	Low	Mouse, Human	mESCs, hiPSCs line (201B7)	Podocytes Tubules (proximal, distal, loop of Henle) Stromal tissue	Complex 3D structure with distinct tissue organization	Kidney development studies	37,35
		Adhesion culture	• Addition of endothelial GF[59] • Automated system[59]	Low	Mouse, Human	mESCs, mESCs line (1B10) hESCs line (H9)	Podocytes Tubules (proximal, distal) Stromal tissue Endothelial tissue	Complex 3D structure with distinct tissue organization	High-throughput screening (HTS)	59–61
		Adhesion and 3D culture: *thick ECM culture*	CRISPR/Cas9[38,63,64]	Low	Human	hESCs line (H9, UM77-2) hiPSCs line (CRL-2522, HDF-α, WTC11, 201B7, WISCi004-A, BCRTi004-A, BCRTi005-A, WA01)	Podocytes Tubules (proximal, distal)	Complex 3D structure with distinct tissue organization	• Kidney development studies • Disease modeling • Drug screening	38,62–65
		Adhesion and 3D culture: *low attachment plate*	• Overexpressed transcription factors[50] • CRISPR/Cas9[66,67,71] • Viral infection[69] • Transplantation[67]	Low	Human	Reprogrammed patient-derived fibroblast, Reprogrammed patient-derived urinary cell, Primary hESCs, hESCs line (H1, H9, HES3, SEES3), hiPSCs line (HDF-α, 201B7, N1/2, CRL-1502, BJFF)	Podocytes Tubules (proximal, distal, loop of Henle, collecting duct) Stromal tissue Endothelial tissue	Complex 3D structure with distinct tissue organization Enter 2nd trimester stage after transplantation	• Kidney development studies • Personalized medicine • Disease modeling • Drug screening • Cell therapy • Transplantation	39,42,50,55,66–71
		Adhesion and 3D culture: *air–liquid interphase*	• Reprogramming cells into PSC[73,74,77] • CRISPR/Cas9[57,58,67,71,74,76] • Transplantation[58,75,76]	Low						40,41,55–58,67,71–77
		Bioreactor	CRISPR/Cas9[78]	Low	Human	hESCs line (H9, hES3), hiPSCs line (MANZ-2, CRL-1502, BJ RiPS)	Podocyte-like Tubules (proximal, distal) Interstitial tissue	Complex 3D structure with distinct tissue organization	• Large-scale organoid production • Disease modeling • Drug screening	78–80

Table 1. Continued

Type of Bioengineered Kidney	Techniques				Cell Sources		Outcomes		Application	Ref.
	Approach	Culture	Combined Method/s	Degree of Modulation*	Organism	Pluripotency	Cell/Tissue Composition	Cells Organization		
		Bioprinting	• CRISPR/Cas9 • Transplantation[76]	Low–moderate	Human	hiPSCs line (CRL-2429)	Podocytes Tubules (proximal, distal, collecting duct) Stromal tissue	Complex 3D structure with distinct tissue organization	• Kidney development studies • Transplantation	57,76
Kidney organoid (glomerulus)	Differentiation of posterior IM with high population of podocyte	Adhesion and 3D culture	• Cell sorting[51] • Enzymatic dissociation[49]	Low–moderate	Human	mESCs (CD1), hiPSCs line (CRL-1502, 201B7)	Mono-tissue: Glomeruli Possibly low tubules	Simple complex 3D structure with glomerular tissue	• Kidney development studies • Disease modeling • Drug screening	49,51
Kidney organoid (tubular)	Differentiation of posterior IM with high population of tubular cells	Adhesion and 3D culture	Cell sorting	Low–moderate	Mouse, Human	mESCs, fetal human fibroblast, hESCs line (KhES-1)	Tubules (proximal, distal, loop of Henle, collecting duct)	Complex 3D with tubular structure	• Kidney development studies • Disease modeling • Drug screening • Cell therapy	48
	Direct epithelial differentiation from fibroblast	Adhesion and 3D culture	• Overexpressed transcription factors • Recellularization on kidney scaffold	Low–moderate	Mouse, Human	mESC (Gt(ROSA)26S) Reprogrammed human fibroblast	Tubules (proximal, distal, loop of Henle)			47
Kidney in scaffolds	Scaffolds mediate 3D organization	Kidney tubules in casting mold	Fabrication of: • Molten agar mold[82] • PDMS mold[83]	Low–moderate	Rat, Human Canine, Human	*PSCs:* rESC, patient-derived hiPSCs *Adult cells:* Human ADPKD cells, tubular cell line (MDCK)	Podocyte-like tubules UB: UB tree	3D structure with distinct tissue organization 3D structure organized in tubular structure	• Tissue-organ reconstruction • Drug screening • Transplantation	82,83
		Kidney tubules in hollow fiber	• Dry-wet processing[84] • Electrospinning[85,86]	Moderate–high	Canine, Human	tubular cell line (PTEC, HK-2, MDCK)	Tubules	3D structure organized in tubular structure		84–86
		Kidney tubules and organdies in porous scaffold	• Electrospinning[87] • Porogen technique[88,89]	Moderate–high	Human	tubular cell line (RC-124, HRCE), carcinoma *PSCs:* hiPSCs line (WTC11)	Tubules Podocytes Tubules (proximal, distal, collecting duct)	3D structure possibly tubular Complex 3D structure with distinct tissue organization. Possibly with vascularization		29,87–89,90
Kidney-on-a-chip	Fluidic system	Glomerulus-on-a-chip	• Soft lithography • Coculture with endothelial cells	Moderate–high	Human	*PSCs:* hESCs line (H9), hiPSCs line (PGP1, IMR-90–1, IISH3i-CB6)	Podocytes Endothelial tissue	2D culture in complex fluidic system	• Tissue–organ reconstruction • Drug screening	91
		Kidney tubules-on-a-chip	• Soft lithography[15] • Bioprinting[14,92] • Coculture with tubular endothelium[15,92]	Moderate–high		*Adult cells:* Primary tubular cell, Tubular carcinoma (A498)	Mono-tissue: proximal tubule	3D tubular structure		14,15,92
		Kidney organoid-on-a-chip	• Bioprinting • Organoid establishment	Moderate–high		*PSCs:* hESCs line (H9, BJFF)	Podocytes Tubules (proximal, distal, loop of Henle)	Complex 3D structure with distinct tissue organization and vascularization		93

*Processes required until completion of bioengineered kidney model.

Despite the aforementioned limitations, the knowledge obtained from studies employing decellularization and recellularization of kidneys is useful for the establishment and optimization of other 3D bioengineered kidney models.

Reaggregation of Kidney Cells

While the decellularized scaffolds might have supported 3D tissue structures, 14 studies attempted to generate kidney tissues via the cellular intrinsic capacity to self-assemble in 3D culture. We distinguish these studies from kidney organoids because adult kidney cells were used instead of stem cells. Primary cells, cell lines obtained from healthy kidneys, or kidney cell carcinoma were employed for reaggregation. We found 3 different methods to reaggregate cells in vitro and summarized them below:

Direct Aggregation (2 Studies)

Cells of single-cell suspension possess the ability to self-assemble and to form spheroids if cultured on low adhesion plates. Two studies took advantage of this characteristic.[9,32] Minced whole kidney tissue obtained from donors were utilized as the cell source in each case. However, these primary aggregates (passage 1) could also be dissociated again and secondary aggregates (passage 2) could be formed from the primary aggregate-derived cells. Buzhor et al. found in this regard that spheroids generated from higher passages displayed a more sphere-like morphology.[32]

Hanging Drop Method (2 Studies)

The hanging drop approach, which is a rather rare method because of its challenging implementation, forms cellular aggregates as gravity acts on single cells suspended in droplets hanging at the bottom side of culture plate covers. Here, the concentration and amount of the primary cells per spheroid could precisely be adjusted. A density of 8×10^3 cells/droplet appeared to be the optimal size to exhaust proliferation capacity.[11,33] In the present studies, solubilized human and porcine renal tissue ECM were added to the culture media to provide all important factors that may support renal cell function.

Aggregates in Gels (10 Studies)

In order to facilitate self-aggregation, a 3D environment is preferentially provided in the form of gels to simulate the native kidney ECM. In this regard, the most commonly employed gels were Matrigel only,[8,16,17,34] Matrigel mixed with collagen,[12,13] basement membrane extract,[11] and hydrogels.[34–36] Hydrogels used in these studies were poly(ethylene glycol)[34] based and hyaluronic acid[34–36] based. Additionally, one study generated cell aggregates in a hydrogel based on kidney ECM-derived bioink.[31] As bioprinted renal constructs not only exhibited structural and functional similarities to the native kidney tissue but also enhanced cellular maturation and tissue formation, it seems advantageous to provide kidney-specific ECM. The use of the kidney ECM-derived hydrogel, however, raised the potential problem of fibrosis as confirmed by magnified TGF-β1 concentration.

Most studies suspended single cells,[12,13,31,34] cell pellets,[8,10,16] or tissue fragments[16,35,36] in the gel substrate/bioink before the gelation process started. Only 2 studies cultured a single-cell suspension[17] or cell pellets[8] on top of a Matrigel layer in order to initiate the formation of 3D tissue. Cell sources were rather various ranging from highly purified human renal proximal tubule epithelial cells[17,34] over human primary renal cortical cells/tissue fragments[12,13,16,31,34,35] to cells derived from minced human adult whole kidney tissue.[8]

Gels were also frequently utilized to generate kidney tubular structures in cell aggregates.[8,12,13,16,17,31,34–36] In this regard, tubular fragments extracted from native kidneys and incorporated within Matrigel formed so-called tubuloids containing primary kidney tubular epithelial cells representing proximal as well as distal nephron segments.[16] Another group systematically investigated the ability of different hydrogel properties to regulate renal tubulogenesis with single cells suspended in a tuneable 3D hydrogel model.[34] Tubules of both studies exhibited apicobasal polarity[16,34] comparable to native kidney tubules.[16] In contrast, mixed human kidney cells as well as primary renal proximal tubular epithelial cells formed dome-like tubulocystic configurations with central lumens, called tubulocysts. Based on this, the authors assumed some sort of solute transport and water influx occurring here.[8]

Kidney Organoid

Kidney organoids have already been generated from PSCs via directed differentiation.[37–43] The differentiation protocols mimic the steps of in vivo kidney development to generate ureteric bud (UB) and nephron progenitor cells (NPCs). While UBs are derived from anterior intermediate mesoderm (IM), NPCs are derivatives of posterior IM. By following anterior IM differentiation, ureteric bud organoids have been generated from PAX2$^+$ anterior IM cells.[43–46] In contrast, nephron differentiation was demonstrated from different progenitor stages: mesenchyme, IM, and NPCs.[37,39–42] Further, segment-specific induction of glomerular and tubular organoids was also reported.[47–51] One study even used amniotic fluid stem cells to generate nephron organoids.[52]

1. UB Organoids

   Five studies described methods to generate UB organoids from mouse and human PSCs. These studies first induced cells of the primitive streak by activating WNT, BMP, and/or FGF signals. Retinoic acid (RA) was commonly used afterward to induce PAX2$^+$ anterior IM cells.[43,46] Epithelialization of anterior IM cells was facilitated by WNT and FGF signals.[43] The protocols used 2D cultures to induce anterior IM cells, which were subsequently aggregated on low attachment plates to form 3D aggregates.[43–46,53] Matrigel was used to demonstrate the branching morphology of ureteric buds in vitro.[43,46,53] A coculture with mouse embryonic kidneys was performed to facilitate UB network formation.[43,45] Also PSC-derived NPCs were cocultured with UB organoids, which led to the formation of the typical inherent architecture consisting of the peripheral progenitor niche and internally differentiated nephrons interconnected by ureteric epithelium.[43]
2. Nephron Organoids

   We found 34 studies that demonstrated segmented nephron structures consisting of glomeruli, proximal tubules, and distal tubules.[35–40,48,50–75] Most studies followed primitive streak differentiation to induce IM cells that subsequently built segmented nephron structures.[38–42] In this regard, SIX2$^+$ nephron progenitor cells were employed as an indicator for the efficiency of the differentiation into nephrons. Single-cell RNA-seq (scRNA-seq) further confirmed the differentiation into nephron epithelial cells as well as stromal cells and off-target populations.[54,55] Also, batch-to-batch variation was assessed by scRNA-seq, remaining as a major current challenge in kidney organoid research.[56] Furthermore, multiple reporter lines were developed for fate mapping in kidney organoid differentiation.[57] Here, the duration of the exposure to the WNT activator CHIR determined the NPC differentiation into proximal

or distal nephrons.[58] A longer CHIR treatment resulted in more distal nephron compartments, while a shorter treatment induced more proximal nephrons accompanied by more endothelial cells.

Based on culture methods, we found 4 different approaches to generate nephron organoids. Twenty-five studies combined 2D and 3D culture designs during the directed differentiation, while others used direct aggregation (1 study), adhesion culture (3 studies), bioreactors (3 studies), or bioprinting (2 studies). One study showed in vivo differentiation from amniotic fluid stem cells. Here, we summarize all 4 approaches and discuss their advantages and disadvantages.

In Vivo Differentiation (1 Study)

One study used human amniotic fluid stem cells (hAFSCs) to generate nephron organoids.[52] hAFSCs were mixed with mESCs in a 1:1 ratio and implanted in athymic rat renal capsule. Transplanted aggregates developed nephron-like structures expressing podocyte and tubular markers.

Embryoid Bodies (2 Studies)

3D aggregates were formed from pluripotent cells on low adhesion 96-well plates and subsequently differentiated into metanephric mesenchyme cells following a 5-step differentiation protocol. Differentiated aggregates were transferred onto a filter afterward and cocultured with mouse embryonic spinal cords. This led to the formation of segmented nephron structures displaying podocytes, proximal tubules, and distal tubules. This study was the first to demonstrate nephron differentiation from mouse and human PSCs.[37,53] However, the requirement of spinal cords was not suited for drug screening in a high-throughput manner.

Adhesion Culture (3 Studies)

In this group, cell differentiation was initiated in a 2D culture (monolayer) on culture plates coated with Geltrex,[59] laminin 521,[60] or gelatin.[61] Cells developed multilayered structures during differentiation, forming nephron structures in thin 3D tissue. A priming step of naive ESCs to epiblast stem cells appeared to help the differentiation into kidney lineages.[61] Adhesion culture is suited for culture automation to perform a high-throughput screening (HTS).[59] This screening experiment further found that VEGF supplementation helped the endothelial differentiation in nephron organoids. While the adhesion culture approach enables automation and screening in a large number, thin 3D tissue might generally not be suited for bioengineering kidney tissues for renal replacement therapies.

Adhesion and 3D Culture (26 Studies)

This approach is the most common one used to generate kidney organoids. Differentiation was initiated in adhesion culture, and differentiated cells were later switched to 3D culture in order to generate thick tissues. Here, the differentiation efficiency appears to be higher using adhesion culture than using the embryoid body approach. This might be due to the equal distribution of GFs to the cells in monolayer cultures. For 3D culture, various culture conditions were employed to form nephron organoids, including the utilization of thick ECM cultures,[38,62–65] U/V-bottom low attachment plates,[39,42,50,55,66–71] and air–liquid interphase cultures.[40,41,55–58,67,71–77] Those approaches can be utilized for drug screening in 96-well plates, yet the medium change in suspension culture can be laborious. A reprogramming approach with synthetic mRNAs of transcription factors (TFs) differentiated hESCs into $SIX2^+SALL1^+$ nephron progenitor cells with an efficiency of up to 92% that also self-differentiated into tubular cells without the additional use of GFs and Matrigel.

The addition of gel to a PSCs suspension showed that the altered ECM stiffness could change the organoid behavior.[67] A hydrogel-based ECM with 1 kPa stiffness is similar to the ECM condition during early differentiation of IM cells in vivo. This condition enhanced the maturation of nephron organoids as shown by a 2–3 times higher percentage of $WT1^+NPHS1^+LTL^+$ cells than those in 60 kPa stiffness. Little is known about the significance of soft gel utilization compared with free-gel environments. Further investigations on the effects of gel components, stiffness, and differentiation signals might provide a better understanding of mechanoresponsive signals during kidney development.

Bioreactor (3 Studies)

The use of a bioreactor may reduce the costs of GFs such as FGF9.[78–80] We found 2 studies that used spinner flasks,[78,80] and 1 study that utilized an orbital shaker with 60 rpm rotation speed.[79] The organoids generated in bioreactors contained $NPHS1^+SYNPO^+$ podocyte-like cells, displaying a decreased expression after treatment with a nephrotoxicant. Interestingly, their composition was dominated by kidney tubules and showed the development of fibrosis. Shear stress might have mediated cellular mechanoresponses that activated apical brush border–related genes, gamma-glutamyl transpeptidase (γ-GT), and sodium–hydrogen exchanger 3.[81] Alternatively, the mechanoresponses could also have accelerated the epithelial-to-mesenchymal transition, a cause of fibrosis.

Bioprinting (2 Studies)

Bioprinting is a recent approach to generate nephron organoids. This technique utilizes a printing syringe to deposit cell aggregates on culture surfaces. It generated cell aggregates at sizes from 5×10^3 to 100×10^3 cells/droplet that were placed on the air–liquid interphase membrane.[57,76] Bioprinting is suited to form organoids in various 3D shapes.

3. Glomerular Organoids

Two studies were focused on glomerular organoid differentiation. These protocols modified the nephron organoid differentiation to enrich the podocyte population:

Adhesion and 3D Culture (2 Studies)

Two studies generated glomerular organoids by 2 different approaches. The first study was to directly differentiate NPCs into podocytes. $ITGA8^+PDGFRa^-$ NPCs were flow-sorted after differentiation by a previously established protocol.[51] The isolated NPCs were reaggregated on a U-bottom low attachment plate before being transferred onto an air–liquid interphase culture. The addition of IWR-1 (Wnt inhibitor) and SB-431542 (TGF-β inhibitor) accelerated the differentiation into $NPHS1^+SYNPO^+$ podocytes with a 65%–95% efficiency. Although the purity was relatively high, podocytes residing in glomerular organoids displayed an inferior $NPHS1^+NPHS2^+$ expression compared with human adult podocytes.

The second approach was to enzymatically dissociate nephron organoids and to capture glomerular structures with the help of a cell strainer.[49] As many as 50–150 glomerular structures were isolated from 1 nephron organoid. Cells were then reaggregated on the low attachment plate to form glomerular organoids consisting of SYNPO$^+$PODXL$^+$ cells. Matrisome analyses showed here maturing components of glomerular basement membranes with Laminin 521 and collagen type IV. The glomerular organoids were further used to model the heterozygous mutation on exon 10 and 27 of *NPHS1* gene, which causes congenital nephrotic syndrome. Concomitantly, glomerular organoids lost podocyte gene expression after 4 days of culture.

4. Tubular Organoids

We found 2 protocols that developed tubular organoids and demonstrated their utility for kidney studies.[47,48] Initially, hESCs were differentiated in 2D culture on culture plates coated with collagen type I. Cells were subsequently harvested and reaggregated on Matrigel to form tubular organoids. Sorting the differentiated cells for kidney-specific cadherin (KSP$^+$/CDH16$^+$) cells enabled to enrich the tubular cell proportion. In parallel, another study used direct reprogramming from fibroblasts to tubular organoids, so called tubuloids.[47] In this regard, mouse fibroblasts were reprogrammed into kidney tubules in Matrigel culture by the overexpression of renal cell fate TFs. These tubuloids showed apicobasal polarity and multiple tubular segments.

Kidney in Scaffolds

Given the essential role of 3D structures and protein matrix compositions, scaffolds are useful to create organized structures in vitro. By designing different shapes of scaffolds, it is possible to modify the 3D structures beyond spheroids. We found 9 studies that engineered kidney tissues within various scaffolds:

Kidney Tubules in Casting Mold (2 Studies)

Molten agar[82] and plastic[83] can be used to generate casting molds. Molds fabricated from matrix proteins including collagen and Matrigel[82] or soft biomaterials such as polydimethyl siloxane (PDMS)[83] permit 3D self-organization and development of kidney tissue. The collagen–Matrigel mold supported the formation of tubule-like structures.[82] It is the high proportion of collagen type I and TGF-β contents in Matrigel that highly likely alters the emergence of tubular structures. A tubular-tree shape of PDMS structure with 700 μm width was successfully reorganized UB tree from various types of cells including MDCK, iPSC, and human ADPKD-derived cells.[83] The UB tree had self-organized 3 h after seeding and formed continuous tubular structures. These structures expressed ureteric tip markers, including PAX2, HOXB7, Claudin 7, and Ret. Nonetheless, the UB-tree tubes had contracted to half of the mold size. The distribution of Ret was obscured and dispersed within the whole structure that appears contrary in comparison to UB organoids that had concentrated Ret expression on the budding tip area.

Kidney Tubules in Hollow Fibers (3 Studies)

We found 2 studies approaching the reconstruction of kidney tubules in hollow fibers using synthetic ECMs. The polyethylene glycol (PEG)[84] and polycaprolactone (PCL)[85,86] based hollow fibers, that were made by dry-wet processing and electrospinning, respectively, were biocompatible with kidney tubular cells. Confluency was confirmed in the PEG hollow fibers after 6 days and tubular brush border enzyme activities could be shown to be accelerated along the increase of the fiber curvature. Limited data showed the polarization and tubular formation inside the fiber. However, tubules in PCL hollow fibers exhibited anion–cations transporters (OAT1, OCT2) expression on basolateral membranes[86] and the capability of secreting uremic toxins.[85]

Kidney Tissues in Porous Scaffold (4 Studies)

This scaffold exhibits a certain plasticity being used for whole kidney tissues mimicking a native decellularized kidney scaffold. The porous area can be achieved by "multiple electrospinning,"[87] the use of porogens such as sodium chloride beads[88] and ice microparticles,[89] or controlled rate freezing.[90] A study using various sizes of PCL fibers generated by multiple electrospinning techniques revealed that fibers with large diameter[87] as well as porosity (~95% with 100–200 μm pore diameter)[87,89] helped kidney cell integration, regardless of the scaffold architecture[87]. The benefit of large pores has also been seen in other biomaterials, including polysaccharides[29] and silk.[88,90] A Matrigel supplementation supported the culture sustainability.[88] These studies also confirmed that porous scaffolds were compatible with not only kidney tubular cell lines[87–89] but also NPCs.[90] A lyophilized silk scaffold was further capable of culturing kidney organoids derived from PSCs, which exhibited vascularization after transplantation underneath a kidney capsule in vivo.[90]

The use of tubular shaped scaffolds appears to be useful for recreating renal tubular structures in vitro. While studies suggested that scaffolds support the maturation of kidney cells, analyses of the underlying mechanism are yet to be performed.

Kidney-on-a-Chip

Organ-on-a-chip models are developed to simulate the in vivo physiological environment by using microfluidic devices. The models typically have 2 channels separated by PDMS membranes to culture epithelial cells and endothelial cells and enable studies investigating their interaction. As kidney-on-a-chip models, we found 5 studies that used typical 2-channel chips to culture podocytes and tubular cells. One study cultured the whole kidney organoids using a fluidic chip without separate channels.

Glomerulus-on-a-Chip (1 Study)

A 2-channel microfluidic device was used to culture podocytes derived from hPSCs.[91] For this, hPSCs were first differentiated into PAX2$^+$WT1$^+$ IM cells and subsequently transferred onto the chip. The IM cells were further directed into NPHS1$^+$ podocytes with a combination of GFs. The primary culture of human glomerular endothelia was seeded on the adjacent channel to simulate the glomerular filtration structure. This system did not have similarly complex capillary loop structures like in vivo glomeruli, yet the 2-channel culture of podocytes and endothelia can be used to study the filtration function of glomeruli in vitro.

Kidney Tubules-on-a-Chip (3 Studies)

Tubules are responsible for the reabsorption of essential nutrients from the primitive urine back to the blood. To simulate the related interaction of tubules and endothelia, tubule-on-a-chip models were developed. For this, tubular structures were created by a bioprinter[14,92] or a PDMS mold.[15] Tubular cells cultured in the columnar-shaped channel exhibited tubular phenotypes of microvilli and brush borders,[14,15,92] as well as water channels,[14] which appeared to be enhanced by a medium perfusion of the lumen. Albumin

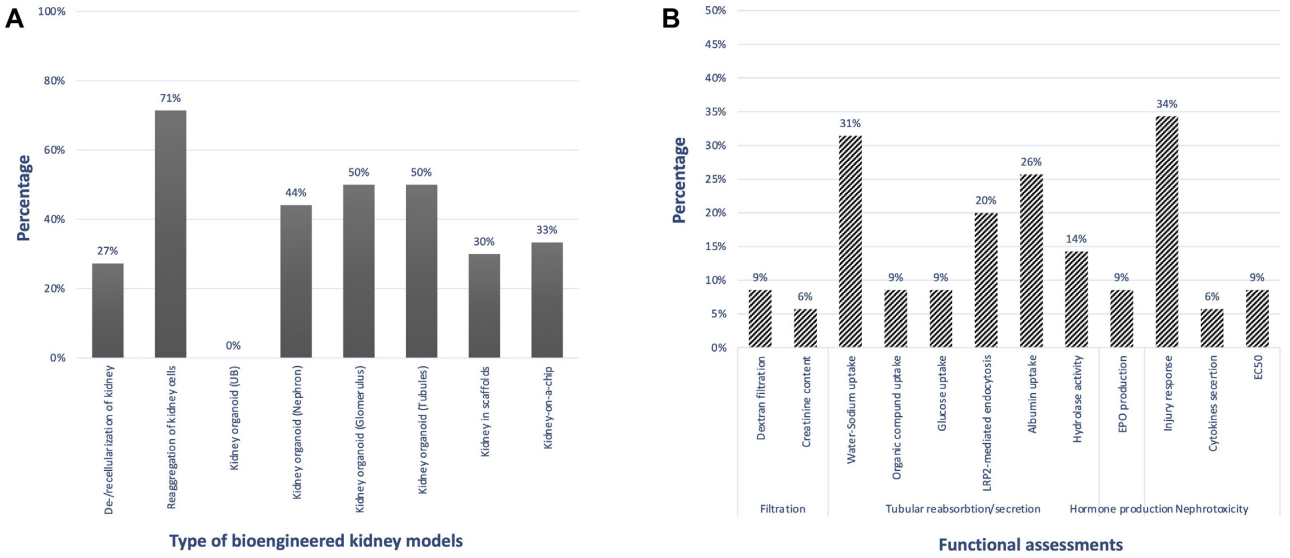

Figure 3. Bioengineered Kidney Models Used for In Vitro Kidney Studies and Their Functional Assessments. **(A)** Percentage of bioengineered kidney models performing functional assessments. **(B)** Percentage of functional assays performed in each type of bioengineered kidney models.

reabsorption was also observed.[15,92] These models would be useful to investigate mechanisms of tubular epithelialization and maturation in 3D tubular structures under flow.

Kidney Organoid-on-a-Chip (1 Study)

One study used whole kidney organoids derived from hPSCs to test fluidic effects on vascularization and nephron maturation.[93] Kidney organoids generated by previously reported protocols[39,42] were transferred onto millifluidic chips and subjected to superfusion of culture media. Vascular formation was enhanced by a high-flow condition, and capillary loop-like structures were observed in ~60% of the organoid glomeruli. Further, cellular polarity of LTL^+ proximal tubules was enhanced, represented by an increased expression of transporter genes. Although the chip model did not allow for the application of a physiological level of shear stress, the study demonstrated the potential of kidney organoids to develop more matured kidney tissue with vasculature in vitro.

Functional Assessments on Bioengineered Kidney Models

To restore the kidney function with bioengineered kidneys, it is necessary to establish adequate methods to evaluate the function of bioengineered kidneys in vitro and in animal models. While all collected studies performed morphological assessments on their kidney models, only 42% of the studies conducted kidney functional assessments. In this regard, reaggregation of kidney cells shows the highest percentage (71%) in testing functionality (Figure 3A). From all physiological assays reported, water-sodium uptake and injury response were the most frequent functional assessments conducted (>30%) (Figure 3B). Here, we summarize all tests for assessing the following kidney functions: glomerular filtration, tubular reabsorption/secretion, hormone production, and nephrotoxicity (Table 2).

Filtration

Dextran Filtration

Glomerular filtration can be tested using various sizes of dextran that is conjugated with fluorescent dyes to evaluate its selectability.[52,58,72] Dextran tests conducted on the filtration barrier in recellularized kidneys[52] and transplanted nephron organoids[58,72] showed a filtration permeability to dextran weighing up to 70 kDa, while no permeability occurred to dextran ≥155 kDa.[52]

Creatinine Content

The kidney is the main route for eliminating creatinine, a protein product released by contracted muscles. Creatinine has a low molecular weight (113 Da), is freely filtered by glomeruli, and secreted by proximal tubules. Creatinine content in the urine decreases significantly in patients with chronic kidney disease and kidney failure.[94] While the assessment of creatinine content is a standard biomarker for a functional kidney in vivo, it can also determine the functionality of bioengineered kidney tissues as reported by 2 studies.[20,72] Creatinine was detected in the tubular fluid in kidney organoids transplanted to the omentum. The creatinine levels were, however, reportedly only half those found in normal urine. This finding suggests that the functional level of bioengineered kidneys still needs to be improved in order to maintain normal homeostasis.[72] In parallel, it could be observed that also recellularized kidneys produce urine with a lower creatinine and urea content than filtrates from the native kidney.[20] Yet, this result needs further validation considering that decellularized kidney scaffolds without residing cells exhibit a low concentration of creatinine and urea.

Given that creatinine is filtered from the blood, this assay is most suitable to test kidney tissues that are exposed to serum or with access to the vessels. Thus, this assay is applicable to test the biological function of transplanted bioengineered kidneys.

Tubular Reabsorption/Secretion

Water Reabsorption and Sodium Uptake

Water transport in the kidney tubules relies on aquaporin activities. Aquaporin 1 (AQP1) is expressed on the apical and basolateral side of proximal tubules,[9,14,48,50,92] while aquaporin 2 (AQP2) is expressed in connecting tubules and collecting ducts.[9,48,60,75] A quantitative assessment of water reabsorption is quite common in the in vivo kidney by

Table 2. Reported Studies That Performed Designated Functional Assays on Their Bioengineered Kidney Models

Type of Functional Assessments	Assays	Parameters	Responsive Cells/Tissues in Bioengineered Kidney	Ref.	Bioengineered Kidney Model*
Filtration	Dextran filtration	Various sizes of fluorescence dextran Up to 70 kDa	Podocytes	52,58,72	De-/recellularization of kidney Kidney organoid (nephron)
	Creatinine content	Colorimetric detection	General	20,72	Transplanted recellularized kidney graft Transplanted kidney organoid (nephron)
Tubular reabsorption/secretion	Water reabsorption and sodium uptake	Aquaporins activities AQP1 AQP2	Proximal tubules Distal tubules and collecting duct	9,14,48,50,92 9,48,60,75	Kidney organoid (nephron, tubular) Kidney-on-a-chip
		Sodium transporters activities Na^+/K^+–ATPases Na^+–Cl^- (SCL12A3) Na^+–Pi cotransporter (SLC34A3)	Proximal tubules Distal tubules Proximal tubules	14,20,34,60,92 60,75 17	De-/recellularization of kidney Reaggregation of kidney cells Kidney organoid (nephron) Kidney-on-a-chip
		Sodium fluorescence accumulation (+ inhibitor)	Nephron tubules	24,60	De-/recellularization of kidney Kidney organoid (nephron)
	Organic compound uptake	Organic anion–cation transporters activities OAT1(SLC22A6) OCT2 (SLC22A2) P-gp	Proximal tubules	86,88,96 86 16	Kidney in scaffolds Reaggregation of kidney cells
		Fluorescence organic anion–cation accumulation (+ inhibitor) 6-carboxy fluorescein (6-CF) 4-(4-(dimethylamino)-styryl)-*N*-methylpyridinium iodide (ASP) Rhodamine 123	Proximal tubules	86,88,96 86 16	Kidney in scaffolds Reaggregation of kidney cells

Table 2. Continued

Type of Functional Assessments	Assays	Parameters	Responsive Cells/Tissues in Bioengineered Kidney	Ref.	Bioengineered Kidney Model*
	Glucose uptake	Glucose transporters activities SGLT2 (+ inhibitor)	Proximal tubules	15,69,92	Kidney organoid (nephron) Kidney-on-a-chip
	LRP2-mediated endocytosis	Various sizes of fluorescence dextran (+ inhibitor) 521 Da–70 kDA 521 Da–10 kDa	Proximal tubules Distal tubules	14,38,40,58,72,78 72	Kidney organoid (nephron) Kidney-on-a-chip
	Albumin uptake	Megalin/LRP2 activities	Proximal tubules	14,15,47,50,60,78,79,88,92	Kidney organoid (nephron, tubular) Kidney-on-a-chip
		Fluorescence albumin accumulation (+ stimulator and inhibitor)	Proximal tubules	14,15,47,50,79,92 97,98	Kidney organoid (nephron, tubular) Kidney-on-a-chip
	Hydrolases activity	Colorimetric detection of: γ-glutamyl transpeptidase (γ-GT) Leucine aminopeptidase (LAP)	Proximal tubules	11,24,33,48,50 24	De-/recellularization of kidney Kidney organoid (nephron, tubular)
Hormone production	EPO production	Colorimetric detection	Kidney tubules	11,24,33	De-/recellularization of kidney
Nephrotoxicity	Injury response	Injury markers activities KIM1 NGAL TUNEL	Proximal tubules Proximal tubules General	35,36,38–40,47,59,80 8,13,35 24,79	Reaggregation of kidney cells Kidney organoid (nephron)
		Protein shedding *N*-acetyl-β-glucosaminidase (NAG) γ-GT	Proximal tubules	35,36 35	Reaggregation of kidney cells
	Pro-inflammatory cytokines secretion	Interleukins (IL-1β, IL-6, IL-8), TNFα, MCP-1, PDGFA content	General	13,80	Reaggregation of kidney cells Kidney organoid (nephron)
	Dose-response survival rate	EC_{50}	General	13,35,36	Reaggregation of kidney cells

*Kidney models tested for functional assay.

measuring urine osmolality, yet scarcely performed in bioengineered kidney tissue. The lack of tubular organization in bioengineered kidneys, however, makes the application of this assay difficult as water is required to pass through the tubule's lumen. But in the majority of the cases, electrolyte uptake can, indeed, estimate the water reabsorption since osmolarity regulation is achieved by balancing the intake and excretion of sodium in the water. Kidney tubules actively reabsorb sodium of which ~70% occurs within the proximal tubules.[95] Many studies evaluated the expression of sodium transporters[14,20,24,34,45,60,75,92] such as Na^+/K^+–ATPases,[14,20,34,60,92] Na^+–Cl^- (SCL12A3),[60,75] and Na^+–Pi (SLC34A3) cotransporters.[17] Some studies further evaluated sodium intracellular uptake using sodium dye that can visualize sodium uptake in kidney tubules.[24,60] The sodium uptake can be inhibited by an Na^+/K^+–ATPase inhibitor, ouabain; statistical analyses on the fluorescent intensity between ouabain-treated and nontreated may therefore further determine the significance of the uptake.[24]

Organic Compounds Uptake

Functional kidney tubules can demonstrate transepithelial transport that employs transporters on the basolateral and apical side. Organic anion transporter (OAT) and organic cation transporter (OCT) are the major transporters expressed on the basolateral side of proximal tubules, pivotal for organic compound transport. OAT1 (SLC22A6) activity can be monitored by adding 6-carboxy fluorescein (6-CF) diacetate, an organic anion substrate, to the culture media. OAT1 hydrolyzes 6-CF diacetate into 6-CF that later is transported intracellularly. Its activity can be inhibited with an OAT1 inhibitor named probenecid, which reduces the accumulation of 6-CF within the cell.[86,88,96] OCT2 (SLC22A2) activity can be evaluated by using 4-(4-(dimethylamino)-styryl)-*N*-methylpyridinium iodide (ASP), a substrate of OCT2. Similar to 6-CF, the fluorescein product of hydrolyzed ASP is also detectable intracellularly. Tetrapentylammonium blocks the OCT2-mediated transport, which can be used to validate the ASP intracellular uptake.[86] In order to evaluate the transepithelial transport via influx and efflux in tubules, fluorescent rhodamine 123 can be used. Following basolateral influx, this fluorescent dye is transported through the apical membrane by *p*-glycoprotein (P-gp). PSC-833, a P-gp inhibitor, reduces the rhodamine efflux toward proximal tubular lumens, which results in fluorescence accumulation on the apical cell membrane.[16]

Glucose Uptake

In the kidney, glucose is freely filtered in the glomeruli and subsequently reabsorbed to the blood circulation by proximal tubules. Sodium-glucose transporter-2 (SGLT2) is a transporter that is expressed on the apical side of proximal tubular cells and plays a pivotal role in glucose reabsorption.[15,70,92] Glucose uptake can be measured quantitatively in kidney tubules-on-a-chip. The addition of dapagliflozin, an SGLT2 inhibitor, reduces the glucose transport from proximal tubules to the vascular lumen.[92]

LRP2-Mediated Endocytosis

Proximal tubules reabsorb proteins via endocytosis that is mediated in part by LRP2, a multiligand binding receptor. In order to test the endocytosis function, varied sizes of dextran can be used. The proximal tubules can endocytose low molecular weight dextran as demonstrated by Lucifer yellow dextran (521 Da) accumulation in previous studies.[38,72] Meanwhile, larger dextrans including 10 kDa[38,40,58,71,78] and 70 kDa[14,58] were detected in the apical intracellular region of proximal tubules.[14,38,40,58,78] The 70 kDa weight was not detected in distal tubules.[72] Latrunculin B, a toxin that blocks actin polymerization, inhibits epithelial endocytosis and thus reduces the dextran accumulation in the proximal tubules.[38] Proximal tubules are, however, unable to endocytose large molecular weight dextran (eg, 2000 kDa).[58] Notably, ARPKD organoids are unable to take up dextran after cyst formation, which can be explained in part by a lack of LRP2 expression on cystic epithelial cells.[58]

Albumin Uptake

Similar to dextran, also albumin undergoes endocytosis through LRP2 in proximal tubules.[95] Bioengineered kidney tissues showed the functionality to reabsorb albumin as reported in previous studies.[14,15,47,50,60,78,79,88,92] Fluorescence-labeled albumin is used to monitor the albumin uptake in functional proximal tubules.[14,15,47,50,79,92]

However, verifying assays of albumin uptake in bioengineered kidney models appeared to be uncommon in previous studies. Assays involving oxidative stress and LRP2 inhibition may validate real-time albumin uptake.[97,98] Oxidative stress reportedly increases the transient expression of LRP2, which can also be caused by high glucose condition as in early stage of diabetes mellitus. The utilization of hydrogen peroxide increases LRP2 expression in a dose- and time-dependent manner, which accelerated the accumulation of fluorescent-labeled albumin in proximal tubular cells.[98] Assays involving leptin, a hormone that correlates with proteinuria in obesity, showed a reduced albumin endocytosis in proximal tubular cells.[97] A leptin concentration of 0.50 μg/mL may potentially be a good concentration for albumin inhibition test.

Hydrolases Activity

Amino acid transport in kidney cells is mainly associated with the activity of cell surface enzymes. To assess this, 3 studies monitored the activity of 2 hydrolases: γ-GT[11,24,33,48,50] and leucine aminopeptidase (LAP),[24] which can be qualitatively assessed by using colorimetric assay. γ-GT and LAP are highly active in kidney tubules as they are pivotal for cysteine and leucine distribution, respectively.[24] In functional proximal tubules, γ-GT actively hydrolyzes L-glutamic-*p*-nitroanilide into *p*-nitroaniline,[11,24,48,50] while LAP hydrolyzes L-leucine-*p*-nitroanilide.[24] The activity of those enzymes is then calculated based on the difference between the absorbance of the substrate and the product.

Hormone Production

Erythropoietin (EPO) Production

EPO is a glycoprotein mainly produced by interstitial cells residing between tubular cells in the adult kidney.[99] The expression of EPO can be detected using EPO marker and immunostaining.[11,24,33] Using ELISA-based assays, EPO production has been measured to confirm the activity of kidney cells in recellularized kidneys[24] and reaggregation of kidney cells models.[11] Considering that EPO is unlikely produced by fetal kidney cells,[99] this assay is better suited as a functional test for bioengineered kidney models that use adult kidney cells.

Nephrotoxicity

Many studies employed their kidney models for toxicity testing including the administration of bacterial Shiga toxins[13]; nanoparticle carriers[36]; cancer and chemotherapy drugs, including SU11274, foretinib,[9] vincristine,[10] cisplatin,[12,35,39,40,47,59,80] and doxorubicin[12,35,49,79]; and nephrotoxic antibiotics/drugs like gentamycin,[12,38,39,47] ampicillin, penicillin,[11] and colchicine.[35]

A toxicity response can be measured using several functional assays:

Injury markers are often used to evaluate nephrotoxicity responses. Kidney injury molecule-1 (KIM1)[35,36,38–40,47,59,80] and neutrophil gelatinase-associated lipocalin (NGAL)[8,13,35] are transmembrane proteins that are responsive to drug-induced inflammation. Further inflammation will lead to kidney cell apoptosis that is represented by TUNEL expression.[24,79] Also, the amount of protein shed in the culture medium such as lysosome enzyme *N*-acetyl-β-glucosaminidase (NAG)[35,36] and γ-GT[35] indicates the level of inflammation. This protein shed had occurred after the introduction of nephrotoxic agents, which is a sign of proximal epithelial cell necrosis.[35,36]

Nephrotoxic agents can also increase the expression of pro-inflammatory cytokines.[13,80] Several cytokines including tumor necrosis factor alpha (TNFα), IL-8, and monocyte chemoattractant protein-1 (MCP-1) were increased in culture medium upon exposure to a toxin.[13] In parallel, cisplatin treatment increased cytokines that are related to chronic kidney injury (IL-8, MCP-1) and renal fibrosis.[80]

During nephrotoxicity tests, cell survival rates can be calculated by determining the half maximal effective concentration (EC_{50}). The EC_{50} value represents the amount of drug or toxic agents that are required to kill 50% of the cells. Three studies utilized EC_{50} to determine the toxicity of their compound on the reaggregation of kidney cells.[11,13,33,35,36]

Generally, functional assessments are more likely to work in bioengineered kidney models that utilize adult renal cells. This tendency explains the reason why functional assessments were mostly conducted in reaggregation kidney cell models that often used adult cells. Mature kidney cells demonstrate kidney function appropriately, even after being transferred to the in vitro environment. Kidney organoids, albeit having more representable tissue organization, are yet to be tested for many of the functional assessments such as the EPO production test. It would be interesting to compare various differentiation protocols for functional assessments to understand possible maturation differences.

Assessments using substrate-conjugated chromophores allow the visible demonstration of physiological processes in kidney tissues. Chromophores also show merit for assessing the function of kidney models in static culture. Meanwhile, the improved tissue organization enables functional assessments beyond the cellular level. The kidney-on-a-chip models, for example, allow the organization of kidney tubules into a solid tubular structure with enhanced maturation. This structure permits assays that rely on the osmolality pressure such as water reabsorption and uptake activities.

Conclusion and Outlook

Bioengineering techniques have been rapidly evolving over the last decade. Initial studies focused on kidney tubular aggregates for various toxicity tests. Later, research focus shifted toward multicellular contexts generated by self-organization of kidney stem cells (eg, kidney organoids), which were used for more translational applications. Also, functional assessments were optimized for their application in in vitro kidney models. Chromophore-based tests are advantageous to evaluate bioengineered kidneys since they provide real-time visualization of kidney function. Notably, the improvement of kidney models may improve the fitness for functional assessments. Overall, a large proportion and diversification of physiology assessments contribute to the rapid improvement of biologically relevant kidney models for various kidney studies.

Acknowledgment

Figure 2 was partially created with BioRender.com.

Conflict of Interest

None declared.

Data Availability

No new data were generated or analyzed in support of this research.

References

1. Duval K, Grover H, Han L, et al. Modeling physiological events in 2D vs. 3D cell culture. *Physiology (Bethesda)* 2017;**32**(4):266–277.
2. Clevers H. Modeling development and disease with organoids. *Cell* 2016;**165**(7):1586–1597.
3. Artegiani B, Clevers H. Use and application of 3D-organoid technology. *Hum Mol Genet* 2018;**27**(R2):R99–R107.
4. Rossi G, Manfrin A, Lutolf MP. Progress and potential in organoid research. *Nat Rev Genet* 2018;**19**(11):671–687.
5. de Souza N. Organoids. *Nat Methods* 2018;**15**(1):23.
6. Miyoshi T, Hiratsuka K, Saiz EG, et al. Kidney organoids in translational medicine: disease modeling and regenerative medicine. *Dev Dyn* 2020;**249**(1):34–45.
7. Du C, Narayanan K, Leong MF, et al. Functional kidney bioengineering with pluripotent stem-cell-derived renal progenitor cells and decellularized kidney scaffolds. *Adv Healthc Mater* 2016;**5**(16):2080–2091.
8. Jun DY, Kim SY, Na JC, et al. Tubular organotypic culture model of human kidney. *PLoS One* 2018;**13**(10):e0206447.
9. Grassi L, Alfonso R, Francescangeli F, et al. Organoids as a new model for improving regenerative medicine and cancer personalized therapy in renal diseases. *Cell Death Dis* 2019;**10**(3):201.
10. Calandrini C, Schutgens F, Oka R, et al. An organoid biobank for childhood kidney cancers that captures disease and tissue heterogeneity. *Nat Commun* 2020;**11**(1):1310.
11. Ding B, Sun G, Liu S, et al. Three-dimensional renal organoids from whole kidney cells: generation, optimization, and potential application in nephrotoxicology in vitro. *Cell Transplant* 2020;**29**:963689719897066.
12. DesRochers TM, Suter L, Roth A, et al. Bioengineered 3D human kidney tissue, a platform for the determination of nephrotoxicity. *PLoS One* 2013;**8**(3):e59219.
13. DesRochers TM, Kimmerling MP, Jandhyala DM, et al. Effects of Shiga toxin type 2 on a bioengineered three-dimensional model of human renal tissue. *Infect Immun* 2015;**83**(1);28–38.
14. Homan KA, Kolesky DB, Skylar-Scott MA,,, et al. Bioprinting of 3D convoluted renal proximal tubules on perfusable chips. *Sci Rep* 2016;**6**(1):34845.
15. Rayner SG, Phong KT, Xue J, et al. Reconstructing the human renal vascular–tubular unit in vitro. *Adv Healthc Mater* 2018;**7**(23):e1801120.

16. Schutgens F, Rookmaaker MB, Margaritis T, et al. Tubuloids derived from human adult kidney and urine for personalized disease modeling. *Nat Biotechnol* 2019;**37**(3):303–313.
17. Xia S, Wu M, Chen S, et al. Long term culture of human kidney proximal tubule epithelial cells maintains lineage functions and serves as an ex vivo model for coronavirus associated kidney injury. *Virol Sin* 2020;**35**(3):311–320
18. Jourde-Chiche N, Fakhouri F, Dou L, et al. Endothelium structure and function in kidney health and disease, *Nat Rev Nephrol* 2019;**15**(2):87108.
19. Moher D, Liberati T, Tetzlaff J, et al. Preferred reporting items for systematic reviews and meta-analyses: the PRISMA statement. *PLoS Med* 2009;**6**(7):e1000097.
20. Song JJ, Guyette JP, Glipin SE, et al. Regeneration and experimental orthotopic transplantation of a bioengineered kidney. *Nat Med* 2013;**19**(5):646–651.
21. Yu YL, Shao YK, Ding YQ, et al. Decellularized kidney scaffold-mediated renal regeneration. *Biomaterials* 2014;**35**(25):6822–6828.
22. Ciampi O, Bonandrini B, Derosas M, et al. Engineering the vasculature of decellularized rat kidney scaffolds using human induced pluripotent stem cell-derived endothelial cells. *Sci Rep* 2019;**9**(1):8001.
23. Guan Y, Liu S, Liu Y, et al. Porcine kidneys as a source of ECM scaffold for kidney regeneration. *Mater Sci Eng C Mater Biol Appl* 2015;**56**:451–456.
24. Abolbashari M, Agcaoili SM, Lee MK, et al. Repopulation of porcine kidney scaffold using porcine primary renal cells. *Acta Biomater* 2016;**29**:52–61.
25. Fischer I, Westphal M, Rossbach B, et al. Comparative characterization of decellularized renal scaffolds for tissue engineering. *Biomed Mater* 2017;**12**(4):045005.
26. Hussein KH, Saleh T, Ahmed E, et al. Biocompatibility and hemocompatibility of efficiently decellularized whole porcine kidney for tissue engineering. *J Biomed Mater Res A* 2018;**106**(7):2034–2047.
27. Kajbafzadeh AM, Khorramirouz R, Nabavizadeh B, et al. Whole organ sheep kidney tissue engineering and in vivo transplantation: effects of perfusion-based decellularization on vascular integrity. *Mater Sci Eng C Mater Biol Appl* 2019;**98**;392–400.
28. Nakayama KH, Lee CC, Batchelder CA, et al. Tissue specificity of decellularized rhesus monkey kidney and lung scaffolds. *PLoS One* 2013;**8**(5):e64134.
29. Batchelder CA, Martinez ML, Duru M, et al. Three-dimensional culture of human renal cell carcinoma organoids. *PLoS One* 2015;**10**(8):e0136758.
30. Peloso A, Ferrario J, Maiga B, et al. Creation and implantation of acellular rat renal ECM-based scaffolds. *Organogenesis* 2015;**11**(2):58–74.
31. Ali M, Pr AK, Yoo JJ, et al. A photo-crosslinkable kidney ECM-derived bioink accelerates renal tissue formation. *Adv Healthc Mater* 2019;**8**(7):e1800992.
32. Buzhor E, Harari-Steinberg O, Omer D, et al. Kidney spheroids recapitulate tubular organoids leading to enhanced tubulogenic potency of human kidney-derived cells. *Tissue Eng Part A* 2011;**17**(17–18):2305–2319.
33. Sun G, Ding B, Wan M, et al. Formation and optimization of three-dimensional organoids generated from urine-derived stem cells for renal function in vitro. *Stem Cell Res Ther* 2020;**11**(1):309.
34. Weber HM, Tsurkan MV, Magno V, et al. Heparin-based hydrogels induce human renal tubulogenesis in vitro. *Acta Biomater* 2017;**57**:59–69.
35. Astashkina AI, Mann BK, Prestwich GD, et al. Comparing predictive drug nephrotoxicity biomarkers in kidney 3-D primary organoid culture and immortalized cell lines. *Biomaterials* 2012;**33**(18):4712–4721.
36. Astashkina AI, Jones CF, Thiagarajan G, et al. Nanoparticle toxicity assessment using an in vitro 3-D kidney organoid culture model. *Biomaterials* 2014;**35**(24):6323–6331.
37. Taguchi A, Kaku Y, Ohmori A, et al. Redefining the in vivo origin of metanephric nephron progenitors enables generation of complex kidney structures from pluripotent stem cells. *Cell Stem Cell* 2014;**14**(1):53–67.
38. Freedman BS, Brooks CR, Lam AQ, et al. Modelling kidney disease with CRISPR-mutant kidney organoids derived from human pluripotent epiblast spheroids. *Nat Commun* 2015;**6**(1):8715.
39. Morizane R, Lam AQ, Freedman BS, et al. Nephron organoids derived from human pluripotent stem cells model kidney development and injury. *Nat Biotechnol* 2015;**33**(11):1193–1200.
40. Takasato M, Er PX, Chiu HS, et al. Kidney organoids from human iPS cells contain multiple lineages and model human nephrogenesis. *Nature* 2015;**526**(7574):564–568.
41. Takasato M, Er PX, Chiu HS, et al. Generation of kidney organoids from human pluripotent stem cells. *Nat Protoc* 2016;**11**(9):1681–1692.
42. Morizane R, Bonventre JV. Generation of nephron progenitor cells and kidney organoids from human pluripotent stem cells. *Nat Protoc* 2017;**12**(1):195–207.
43. Taguchi A, Nishinakamura R. Higher-order kidney organogenesis from pluripotent stem cells. *Cell Stem Cell* 2017;**21**(6):730.e6–746.e6.
44. Chang CH, Davies JA. An improved method of renal tissue engineering, by combining renal dissociation and reaggregation with a low-volume culture technique, results in development of engineered kidneys complete with loops of Henle. *Nephron Exp Nephrol* 2012;**121**(3–4):e79–e85.
45. Xia Y, Sancho-Martinez I, Nivet E, et al. The generation of kidney organoids by differentiation of human pluripotent cells to ureteric bud progenitor-like cells. *Nat Protoc* 2014;**9**(11):2693–2704.
46. Mae SI, Ryosaka M, Toyoda T, et al. Generation of branching ureteric bud tissues from human pluripotent stem cells. *Biochem Biophys Res Commun* 2018;**495**(1):954–961.
47. Kaminski MM, Tosic J, Kresbach C, et al. Direct reprogramming of fibroblasts into renal tubular epithelial cells by defined transcription factors. *Nat Cell Biol* 2016;**18**(12):1269–1280.
48. Yamaguchi S, Morizane R, Homma K, et al. Generation of kidney tubular organoids from human pluripotent stem cells. *Sci Rep* 2016;**6**(1):38353.
49. Hale LJ, Howden SE, Phipson B, et al. 3D organoid-derived human glomeruli for personalised podocyte disease modelling and drug screening. *Nat Commun* 2018;**9**(1):5167.
50. Hiratsuka K, Monkawa T, Akiyama T, et al. Induction of human pluripotent stem cells into kidney tissues by synthetic mRNAs encoding transcription factors. *Sci Rep* 2019;**9**(1):913.
51. Yoshimura Y, Taguchi A, Tanigawa S, et al. Manipulation of nephron-patterning signals enables selective induction of podocytes from human pluripotent stem cells. *J Am Soc Nephrol* 2019;**30**(2):304–321.
52. Xinaris C, Benedetti V, Novelli R, et al. Functional human podocytes generated in organoids from amniotic fluid stem cells. *J Am Soc Nephrol* 2016;**27**(5):1400–1411.

53. Kuraoka S, Tanigawa S, Taguchi A,,, et al. *PKD1*-dependent renal cystogenesis in human induced pluripotent stem cell-derived ureteric bud/collecting duct organoids. *J Am Soc Nephrol* 2020;**31**(10):2355–2371.
54. Wu H, Uchimura K, Donnelly EL, et al. Comparative analysis and refinement of human PSC-derived kidney organoid differentiation with single-cell transcriptomics. *Cell Stem Cell* 2018;**23**(6):869.e8–881.e8.
55. Subramanian A, Sidhom EH, Emani M, et al. Single cell census of human kidney organoids shows reproducibility and diminished off-target cells after transplantation. *Nat Commun* 2019;**10**(1):5462.
56. Phipson B, Er PX, Combes AN, et al. Evaluation of variability in human kidney organoids. *Nat Methods* 2019;**16**(1):79–87.
57. Howden SE, Vanslambruock JM, Wilson SB, et al. Reporter-based fate mapping in human kidney organoids confirms nephron lineage relationships and reveals synchronous nephron formation. *EMBO Rep* 2019;**20**(4):e47483.
58. Low JH, Li P, Chew EGY, et al. Generation of human PSC-derived kidney organoids with patterned nephron segments and a de novo vascular network. *Cell Stem Cell* 2019;**25**(3):373.e9–387.e9.
59. Czerniecki SM, Cruz NM, Harder JL, et al. High-throughput screening enhances kidney organoid differentiation from human pluripotent stem cells and enables automated multidimensional phenotyping. *Cell Stem Cell* 2018;**22**(6):929.e4–940.e4.
60. Hariharan K, Stachelscheid H, Rossbach B, et al. Parallel generation of easily selectable multiple nephronal cell types from human pluripotent stem cells. *Cell Mol Life Sci* 2019;**76**(1):179–192.
61. Chow T, Wong FTM, Monetti C, et al. Recapitulating kidney development in vitro by priming and differentiating mouse embryonic stem cells in monolayers. *NPJ Regen Med* 2020;**5**(1):7.
62. Cruz NM, Song X, Czerniecki SM, et al. Organoid cystogenesis reveals a critical role of microenvironment in human polycystic kidney disease. *Nat Mater* 2017;**16**(11):1112–1119.
63. Kim YK, Rafaeli I, Brooks CR, et al. Gene-edited human kidney organoids reveal mechanisms of disease in podocyte development. *Stem Cells* 2017;**35**(12):2366–2378.
64. Harder JL, Menon R, Otto EA, et al. Organoid single cell profiling identifies a transcriptional signature of glomerular disease. *JCI Insight* 2019;**4**(1):e122697.
65. Nam SA, Seo E, Kim JW, et al. Graft immaturity and safety concerns in transplanted human kidney organoids. *Exp Mol Med* 2019;**51**(11):1–13.
66. Borestrom C, Jonebring A, Guo J, et al. A CRISP(e)R view on kidney organoids allows generation of an induced pluripotent stem cell-derived kidney model for drug discovery. *Kidney Int* 2018;**94**(6):1099–1110.
67. Tan Z, Shan J, Rak-Raszewska A, et al. Embryonic stem cells derived kidney organoids as faithful models to target programmed nephrogenesis. *Sci Rep* 2018;**8**(1):16618.
68. Garreta E, Prado P, Tarantino C, et al. Fine tuning the extracellular environment accelerates the derivation of kidney organoids from human pluripotent stem cells. *Nat Mater* 2019;**18**(4):397–405.
69. Hollywood JA, Przepiorski A, D'Souza RF, et al. Use of human induced pluripotent stem cells and kidney organoids to develop a cysteamine/mTOR inhibition combination therapy for cystinosis. *J Am Soc Nephrol* 2020;**31**(5):962–982.
70. Monteil V, Kwon H, Prado P, et al. Inhibition of SARS-CoV-2 infections in engineered human tissues using clinical-grade soluble human ACE2. *Cell* 2020;**181**(4);905.e7–913.e7.
71. Shimizu T, Mae SI, Araoka T, et al. A novel ADPKD model using kidney organoids derived from disease-specific human iPSCs. *Biochem Biophys Res Commun* 2020;**529**(4):1186–1194.
72. Li Z, Araoka T, Wu J, et al. 3D culture supports long-term expansion of mouse and human nephrogenic progenitors. *Cell Stem Cell* 2016;**19**(4):516–529.
73. Forbes TA, Howden SE, Lawlor K, et al. Patient-iPSC-derived kidney organoids show functional validation of a ciliopathic renal phenotype and reveal underlying pathogenetic mechanisms. *Am J Hum Genet* 2018;**102**(5):816–831.
74. Tanigawa S, Islam M, Sharmin S, et al. Organoids from nephrotic disease-derived iPSCs identify impaired NEPHRIN localization and slit diaphragm formation in kidney podocytes. *Stem Cell Reports* 2018;**11**(3):727–740.
75. van den Berg CW, Ritsma L, Avramut MC, et al. Renal subcapsular transplantation of PSC-derived kidney organoids induces neo-vasculogenesis and significant glomerular and tubular maturation in vivo. *Stem Cell Reports* 2018;**10**(3):751–765.
76. Vanslambrouck JM, Wilson SB, Tan KS, et al. A toolbox to characterize human induced pluripotent stem cell-derived kidney cell types and organoids. *J Am Soc Nephrol* 2019;**30**(10):1811–1823.
77. Mulder J, Sharmin S, Chow T, et al. Generation of infant- and pediatric-derived urinary induced pluripotent stem cells competent to form kidney organoids. *Pediatr Res* 2020;**87**(4):647–655.
78. Przepiorski A, Sander V, Tran T, et al. A simple bioreactor-based method to generate kidney organoids from pluripotent stem cells. *Stem Cell Reports* 2018;**11**(2):470–484.
79. Kumar SV, Er PX, Lawlor KT, et al. Kidney micro-organoids in suspension culture as a scalable source of human pluripotent stem cell-derived kidney cells. *Development* 2019;**146**(5):dev172361.
80. Digby J, Vanichapol T, Przepiorski A, et al. Evaluation of cisplatin-induced injury in human kidney organoids. *Am J Physiol Renal Physiol* 2020;**318**(4):F971–F978.
81. Ferrell N, Cheng J, Miao S, et al. Orbital shear stress regulates differentiation and barrier function of primary renal tubular epithelial cells. *ASAIO J* 2018;**64**(6):766–772.
82. Lu SH, Lin Q, Liu YN, et al. Self-assembly of renal cells into engineered renal tissues in collagen/Matrigel scaffold in vitro. *J Tissue Eng Regen Med* 2012;**6**(10):786–792.
83. Benedetti V, Brizi V, Guida P, et al. Engineered kidney tubules for modeling patient-specific diseases and drug discovery. *EBioMedicine* 2018;**33**:253–268.
84. Shen C, Meng Q, Zhang G. Increased curvature of hollow fiber membranes could up-regulate differential functions of renal tubular cell layers. *Biotechnol Bioeng* 2013;**110**(8):2173–2183.
85. Jansen J, Fedecostante M, Wilmer MJ, et al. Bioengineered kidney tubules efficiently excrete uremic toxins. *Sci Rep* 2016;**6**(1):26715.
86. Jansen K, Castilho M, Aarts S, et al. Fabrication of kidney proximal tubule grafts using biofunctionalized electrospun polymer scaffolds. *Macromol Biosci* 2019;**19**(2):e1800412.
87. Burton TP, Corcoran A, Callanan A. The effect of electrospun polycaprolactone scaffold morphology on human kidney epithelial cells. *Biomed Mater* 2017;**13**(1):015006.

88. Subramanian B, Rudym D, Cannizzaro C, et al. Tissue-engineered three-dimensional in vitro models for normal and diseased kidney. *Tissue Eng Part A* 2010;**16**(9):2821–2831.
89. Lih E, Park KW, Chun SY, et al. Biomimetic porous PLGA scaffolds incorporating decellularized extracellular matrix for kidney tissue regeneration. *ACS Appl Mater Interfaces* 2016;**8**(33):21145–21154.
90. Gupta AK, Coburn JM, Davis-Knowlton J, et al. Scaffolding kidney organoids on silk. *J Tissue Eng Regen Med* 2019;**13**(5):812–822.
91. Musah S, Dimitrakakis N, Camacho DM, et al. Directed differentiation of human induced pluripotent stem cells into mature kidney podocytes and establishment of a Glomerulus Chip. *Nat Protoc* 2018;**13**(7):1662–1685.
92. Lin NYC, Homan KA, Robinson SS, et al. Renal reabsorption in 3D vascularized proximal tubule models. *Proc Natl Acad Sci USA* 2019;**116**(12):5399–5404.
93. Homan KA, Gupta N, Kroll KT, et al. Flow-enhanced vascularization and maturation of kidney organoids in vitro. *Nat Methods* 2019;**16**(3):255–262.
94. Kashani K, Rosner MH, Ostermann M. Creatinine: from physiology to clinical application. *Eur J Intern Med* 2020;**72**:9–14.
95. Feher J. *Quantitative Human Physiology*. 2nd ed. Cambridge, MA: Academic Press; 2017.
96. Nieskens TT, Peters JG, Schreurs MJ, et al. A human renal proximal tubule cell line with stable organic anion transporter 1 and 3 expression predictive for antiviral-induced toxicity. *AAPS J* 2016;**18**(2):465–475.
97. Briffa JF, Grinfeld E, Mathai ML, et al. Acute leptin exposure reduces megalin expression and upregulates TGFβ1 in cultured renal proximal tubule cells. *Mol Cell Endocrinol* 2015;**5**(401):25–34.
98. Kurosaki Y, Imoto A, Kawakami F, et al. Oxidative stress increases megalin expression in the renal proximal tubules during the normoalbuminuric stage of diabetes mellitus. *Am J Physiol Renal Physiol* 2018;**314**(3):F462–F470.
99. Shih HM, Wu CJ, Lin SL. Physiology and pathophysiology of renal erythropoietin-producing cells. *J Formos Med Assoc* 2018;**117**(11):955–963.